Supporting Information

Alkali Metal Fluorides in Fluorinated Alcohols: Fundamental Properties and Applications to Electrochemical Fluorination

Naoki Shida,[†,‡,] Hiroaki Takenaka,[†] Akihiro Gotou,[#] Tomohiro Isogai,[#] Akiyoshi Yamauchi,[#] Yosuke Kishikawa,[#] Yuuya Nagata,[¶] Ikuyoshi Tomita,[†] Toshio Fuchigami,[†] Shinsuke Inagi[†,§,]**

[†]Department of Chemical Science and Engineering, School of Materials and Chemical Technology, Tokyo Institute of Technology, 4259 Nagatsuta-cho, Midori-ku, Yokohama 226-8502, Japan
Tel: +81-45-924-5407, Fax: +81-45-924-5407

[‡]Department of Chemistry and Life Science, Yokohama National University, 79-5 Tokiwadai, Hodogaya-ku, Yokohama 240-8501, Japan

[#]Daikin Industries Ltd., 1-1 Nishi-Hitotsuya, Settsu, Osaka 566-8585, Japan

[¶]Institute for Chemical Reaction Design and Discovery Hokkaido University Kita 21 Nishi 10, Kita-Ku, Sapporo, Hokkaido 001-0021, Japan

[§]PRESTO, Japan Science and Technology Agency (JST), 4-1-8 Honcho, Kawaguchi, Saitama 332-0012, Japan

E-mail: inagi@cap.mac.titech.ac.jp, shida-naoki-gz@ynu.ac.jp

Table of Contents

1. Potential window analyses

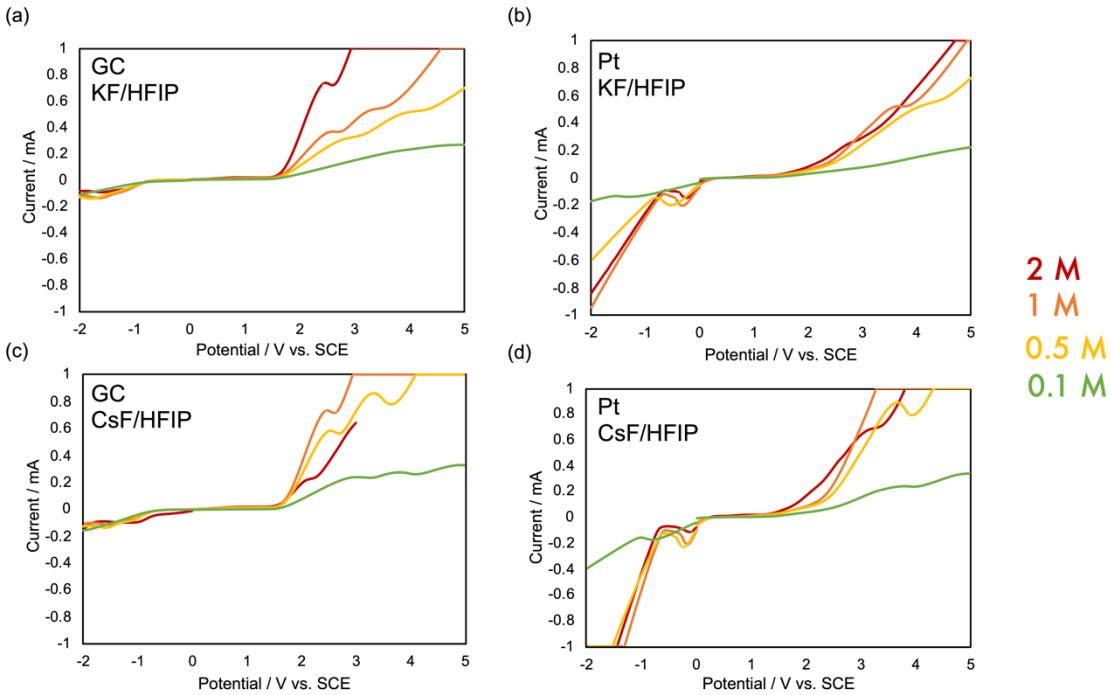

Figure S1. Linear sweep voltammograms of HFIP-based electrolytes using a GC disk or a Pt disk electrode as a working electrode. A Pt-plate counter electrode and a SCE were used as a counter electrode and a reference electrode, respectively. Voltammograms were recorded under ambient conditions at a scan rate of 100 mV/s. (a) KF/HFIP using GC. (b) KF/HFIP using Pt. (c) CsF/HFIP using GC. (d) CsF/HFIP using Pt.

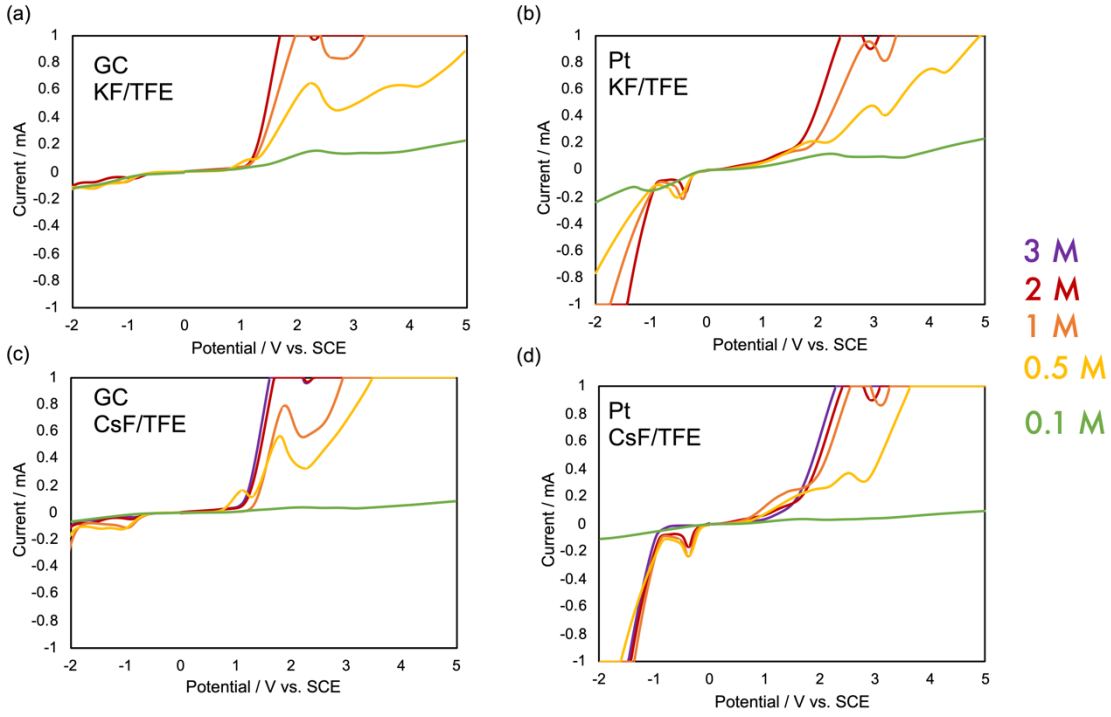

Figure S2. Linear sweep voltammograms of TFE-based electrolytes using a GC disk or a Pt disk electrode as a working electrode. A Pt-plate counter electrode and a SCE were used as a counter electrode and a reference electrode, respectively. Voltammograms were recorded under ambient conditions at a scan rate of 100 mV/s. (a) KF/TFE using GC. (b) KF/TFE using Pt. (c) CsF/TFE using GC. (d) CsF/TFE using Pt.

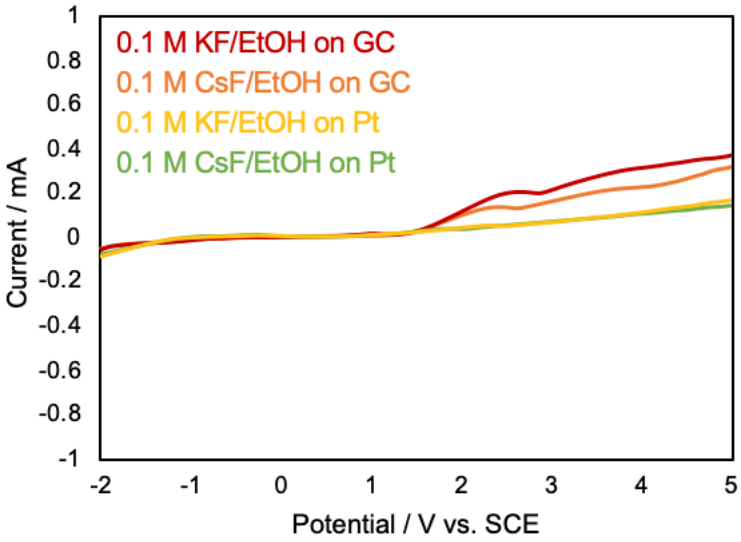

Figure S3. Linear sweep voltammograms of 0.1 M MF/EtOH (M = Cs, K) electrolytes using a GC disk or a Pt disk electrode as a working electrode. A Pt-plate counter electrode and a SCE were used as a counter electrode and a reference electrode, respectively. Voltammograms were recorded under ambient conditions at a scan rate of 100 mV/s.

2. Conductivity of HFIP-containing electrolytes

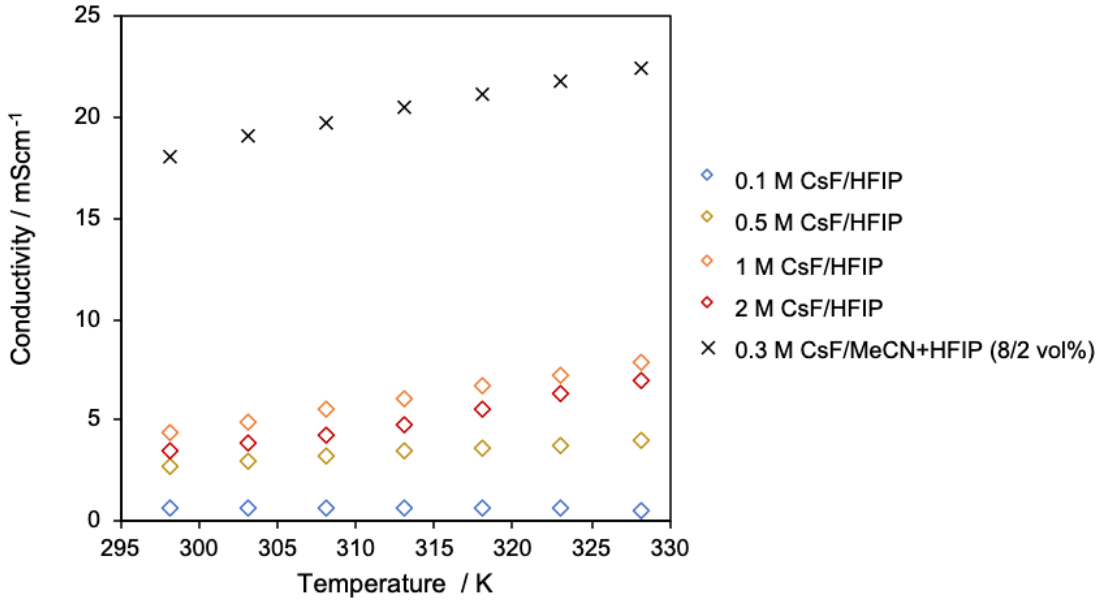

Figure S4. Conductivity of CsF/fluorinated alcohol and 0.3 M CsF/MeCN+HFIP (8/2 vol%) as a function of temperature.

3. Potential window of 0.3 M CsF/MeCN+HFIP (8/2 vol%) electrolyte

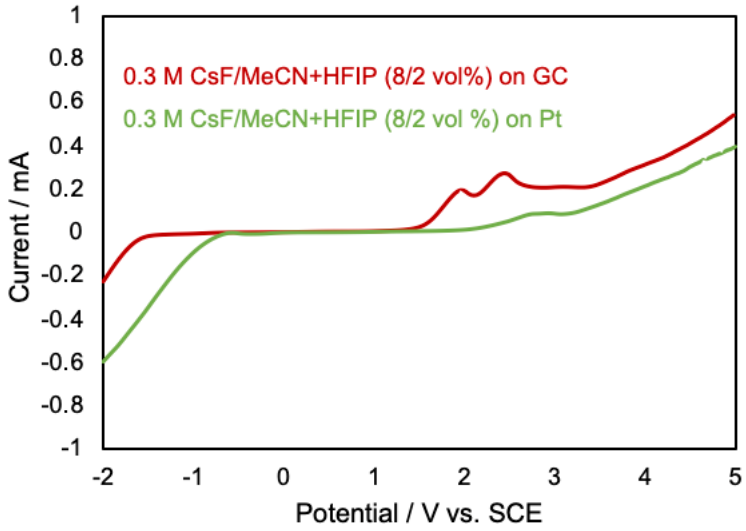

Figure S5. Linear sweep voltammograms of 0.3 M CsF/MeCN+HFIP (8/2) electrolytes using a GC disk or a Pt disk electrode as a working electrode. A Pt-plate counter electrode and a SCE were used as a counter electrode and a reference electrode, respectively. Voltammograms were recorded under ambient conditions at a scan rate of 100 mV/s.

4. Single crystal X-ray diffraction analysis

Table S1. Crystallographic data of CsF-$(HFIP)_3$, CsF-$(TFE)_2$ TBAF-$(TFE)_4$.

Crystal data	**CsF-$(HFIP)_3$**	**CsF-$(TFE)_2$**	**TBAF-$(HFIP)_4$**
CCDC	2067290	2067291	2067292
Empirical Formula	C9H6CsF19O3	C4H6CsF7O2	C24H48F13NO4
Formula Weight	656.05	352.00	661.63
h, k, lmax	11, 24, 13	11, 25, 6	23, 23, 6
Crystal System	orthorhombic	orthorhombic	tetragonal
Space Group	P n m a	P 1 2_1/n 1	I 41/a
a, Å	9.4397(9)	9.4565(8)	19.2444(10)
b, Å	19.928(3)	20.9063(19)	19.2444(10)
c, Å	10.5504(12)	9.7266(10)	9.4489(7)
α, deg	90	90	90
β, deg	90	90	90
γ, deg	90	90	90
Volume, Å	1984.7(4)	1923.0(3)	3499.4(4)
D_{calcd}, g cm^{-3}	2.196	2.432	1.256
Z	4	8	4
F(000)	1240	1312	1392
Data Collection	Data Collection	Data Collection	Data Collection
Temperature, K	93(2)	93(2)	293(2)
2θmax, deg	71.9850	76.4490	73.2350
Tmin/Tmax	0.52422 / 1.0000	0.03095 / 1.0000	0.68094 / 1.0000
Refinement	Refinement	Refinement	Refinement
No. of Observed Data	1994	1971	1741
No. of Parameters	158	139	105
R1[a], wR2[b]	0.1247, 0.3449	0.1455, 0.3310	0.0652, 0.1829
Goodness of Fit Indictor	1.246	1.248	1.120

[a]$R1 = \sum | |Fo| - |Fc| | / \sum |Fo|$ [b]$wR2 = [\sum w ((Fo^2 - Fc^2)^2 / \sum w (Fo^2)^2]^{1/2}$ $w = [\sigma^2(Fo^2)]^{-1}$

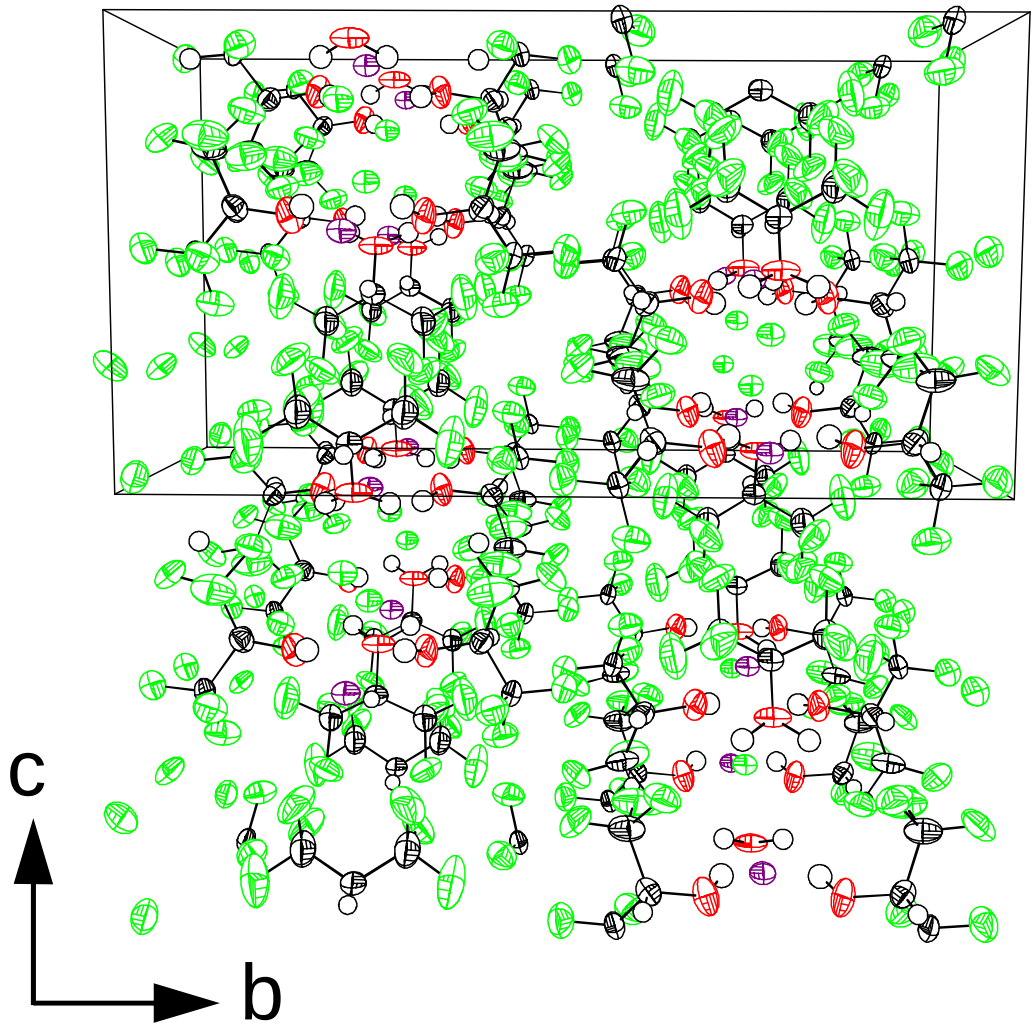

Figure S6. Packing diagram for CsF-$(HFIP)_3$ with anisotropic displacement ellipsoids shown at the 50% probability level. Labelling of atoms is as follows; black: carbon, red: oxygen, green: fluorine, purple: cesium, white: hydrogen.

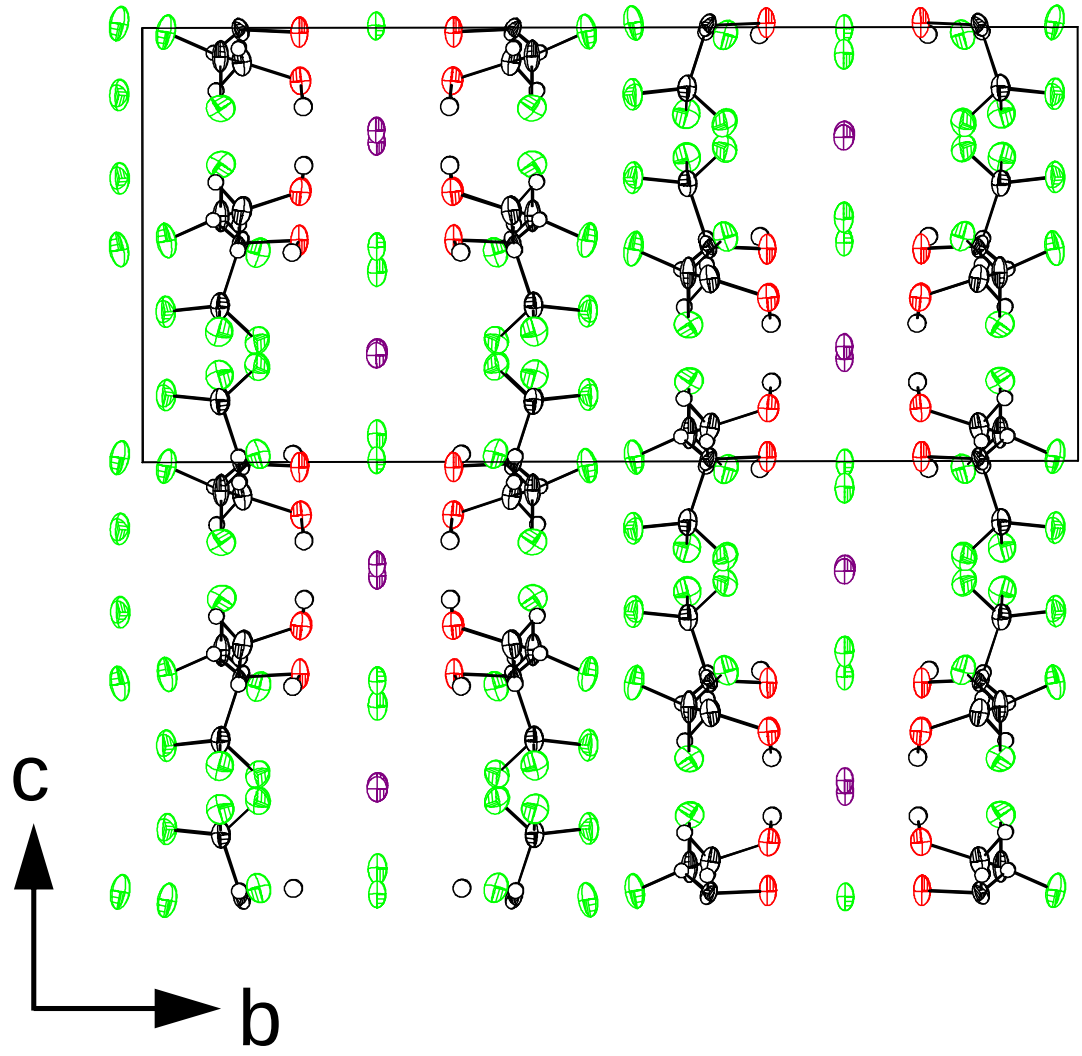

Figure S7. Packing diagram for CsF-$(TFE)_2$ with anisotropic displacement ellipsoids shown at the 50% probability level. Labelling of atoms is as follows; black: carbon, red: oxygen, green: fluorine, purple: cesium, white: hydrogen.

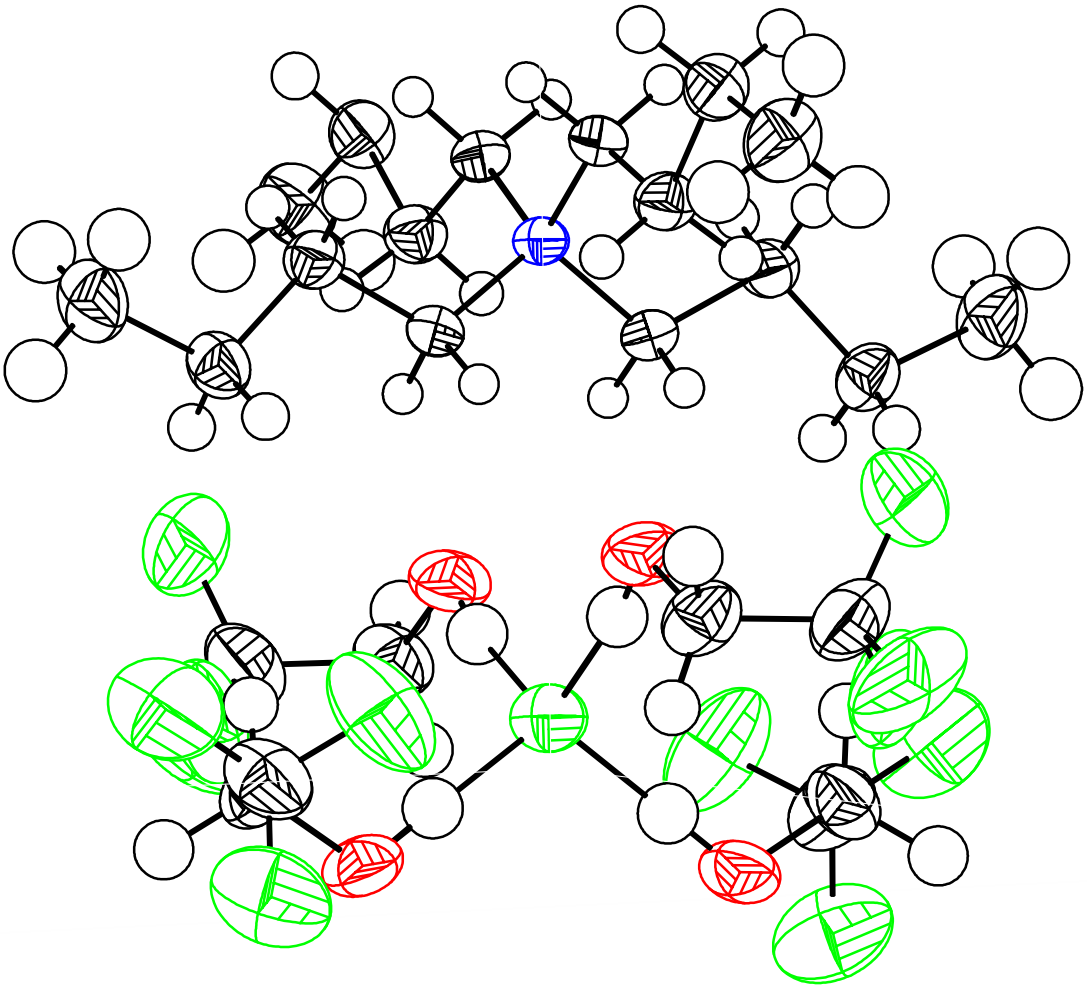

Figure S8. Solid-state structure of TBAF-$(TFE)_4$ with anisotropic displacement ellipsoids shown at the 50% probability level. Labelling of atoms is as follows; black: carbon, red: oxygen, green: fluorine, blue: nitrogen, white: hydrogen.

5. NMR spectra of single crystals

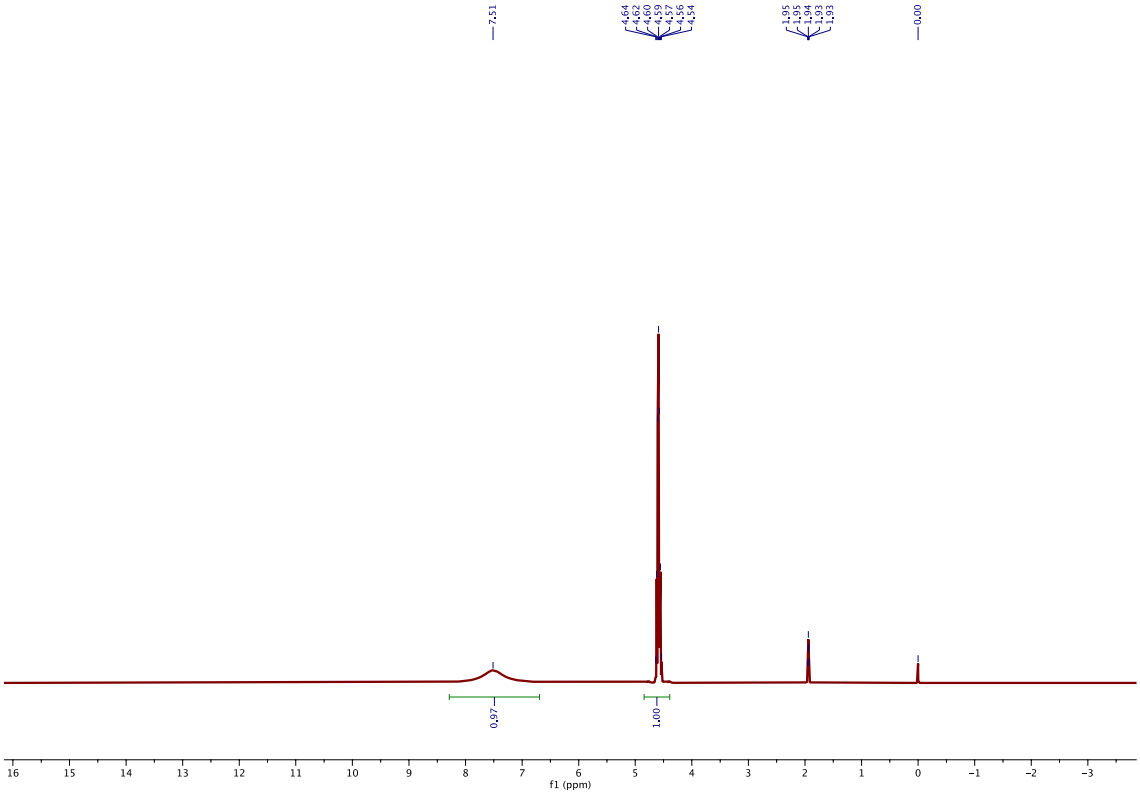

Figure S9. ^{1}H NMR spectrum (400.13 MHz, CD_3CN, 25 °C) of $CsF\text{-}(HFIP)_3$.

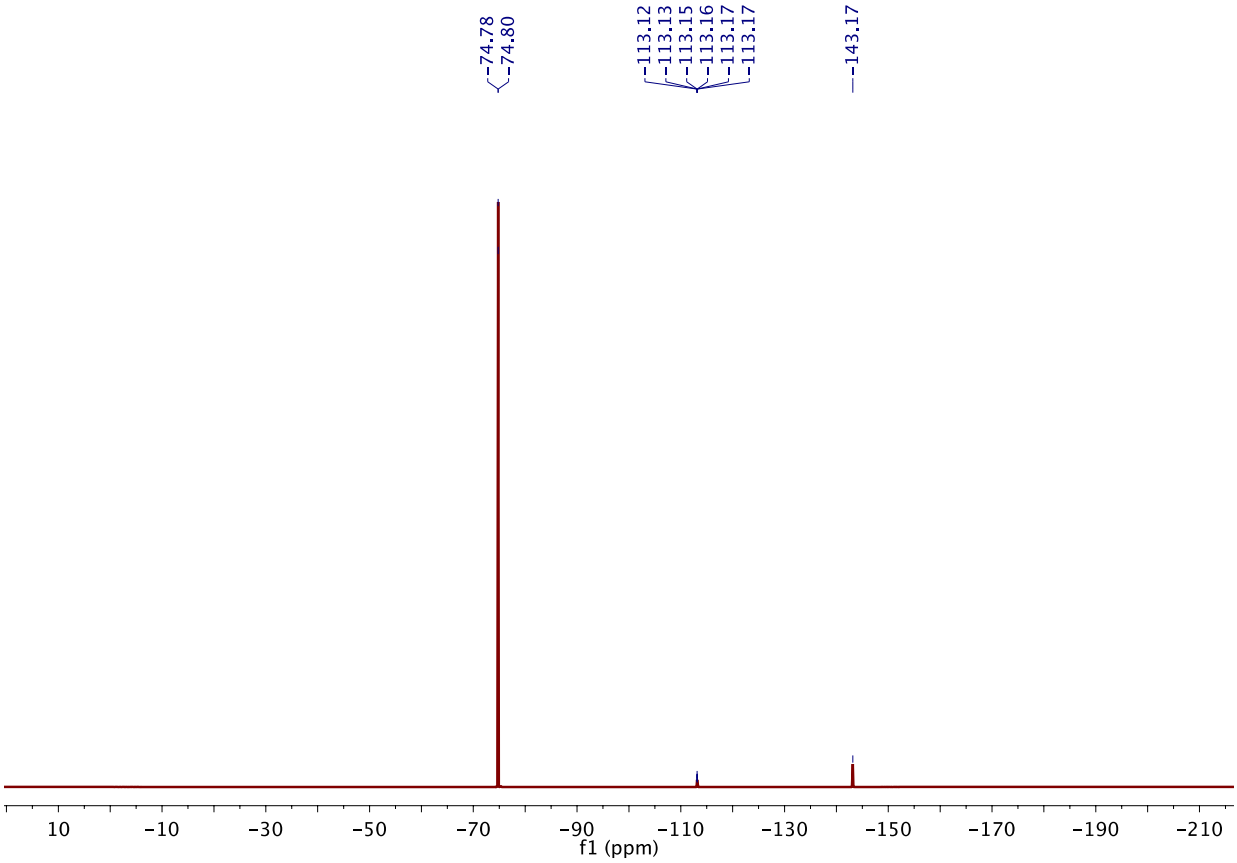

Figure S10. ^{19}F NMR spectrum (376.31 MHz, CD_3CN, 25 °C) of CsF-$(HFIP)_3$.

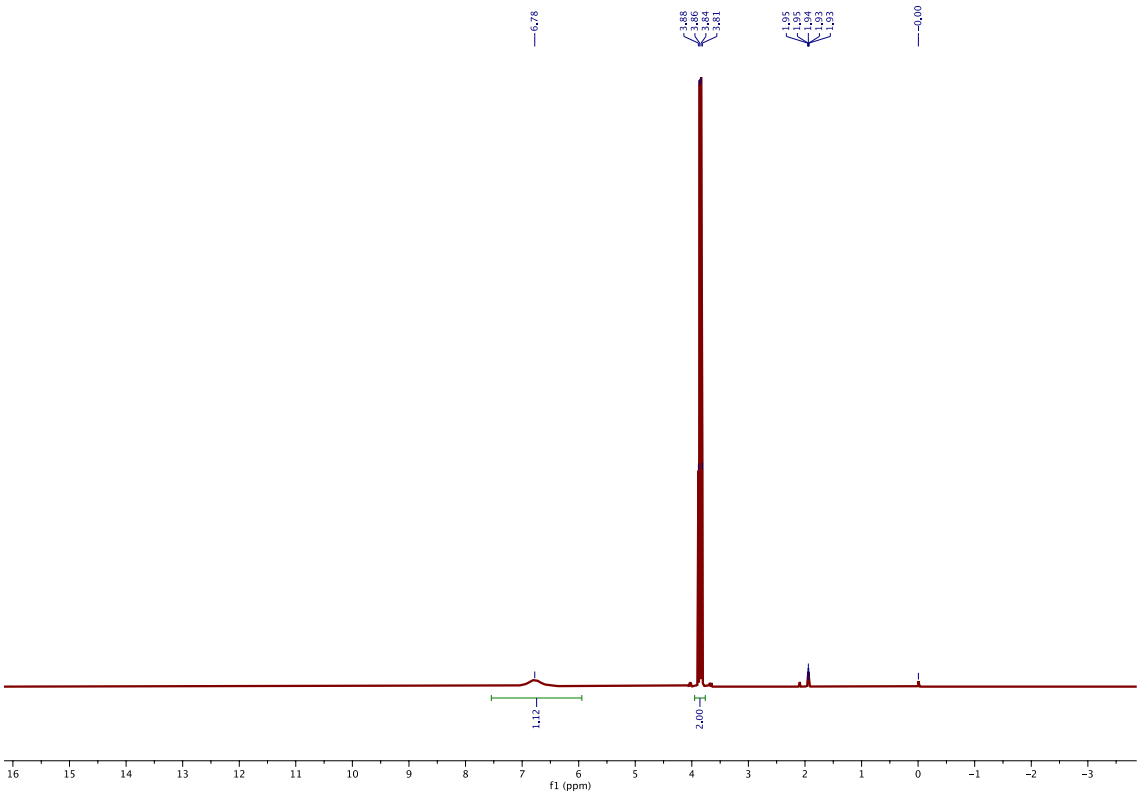

Figure S11. ^{1}H NMR spectrum (400.13 MHz, CD_3CN, 25 °C) of $CsF\text{-}(TFE)_2$.

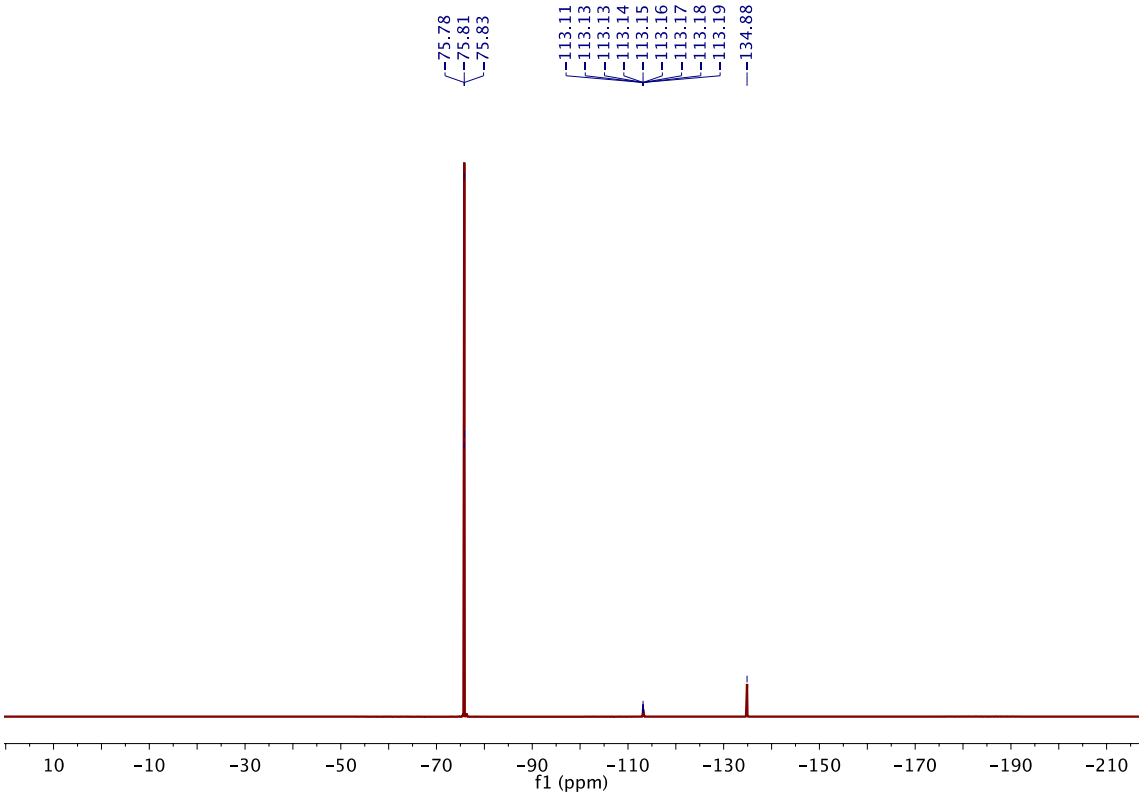

Figure S12. ^{19}F NMR spectrum (376.31 MHz, CD_3CN, 25 °C) of $CsF\text{-}(TFE)_2$.

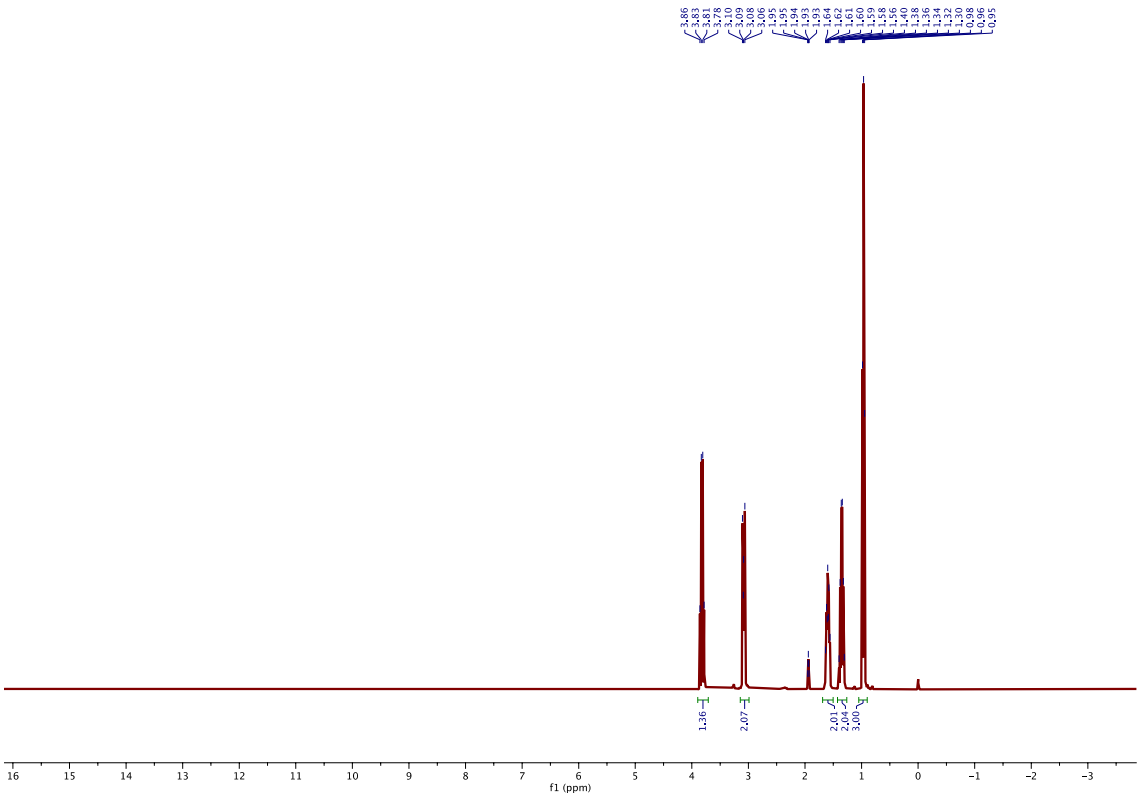

Figure S13. ^{1}H NMR spectrum (400.13 MHz, CD_3CN, 25 °C) of TBAF-$(TFE)_4$.

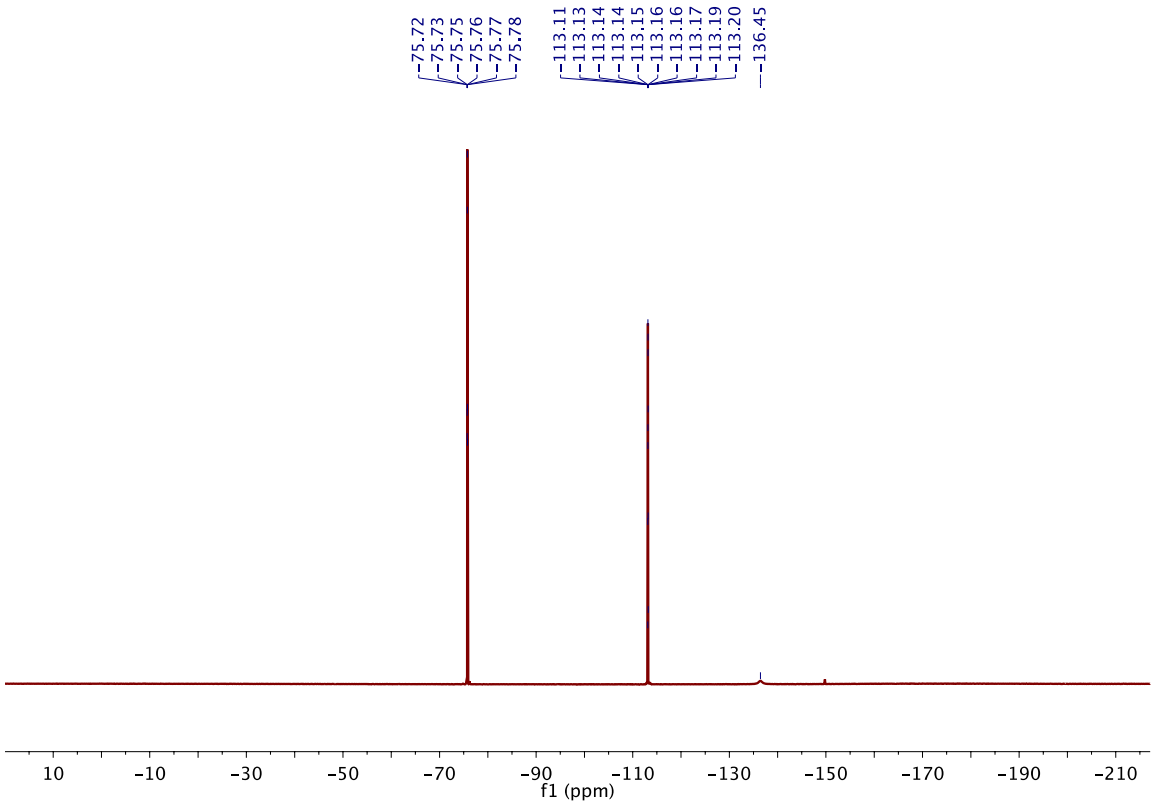

Figure S14. ^{19}F NMR spectrum (376.31 MHz, CD_3CN, 25 °C) of TBAF-$(TFE)_4$.

6. Electrochemical fluorination of triphenylmethane

Table S2. Optimization of reaction conditions for the electrochemical fluorination of triphenylmethane using MF/fluorinated alcohol electrolyte.

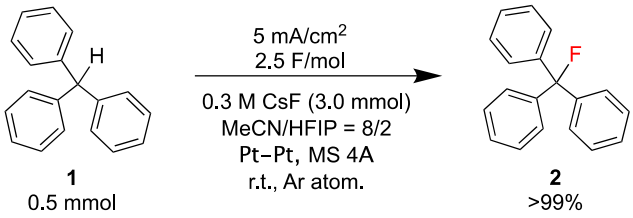

1
0.5 mmol

2
>99%

Entry	Deviation from optimal conditions	Yield [%]
1	none	>99%
2	KF instead of CsF	>99%
3	2.0 F/mol instead of 2.5 F/mol	83%
4	0.1 M CsF instead of 0.3 M CsF	55%
5	HFIP only instead of MeCN/HFIP (8/2)	n.d.
6	TFE (2 mL) instead of HFIP (2 mL)	65%
7	No MS4A	30%
8	Under air	66%
9	GC anode instead of Pt	28%
10	10 mL MeCN with 600 μL of HFIP	84%

7. ^{19}F NMR spectra and GC-MS data for crude materials

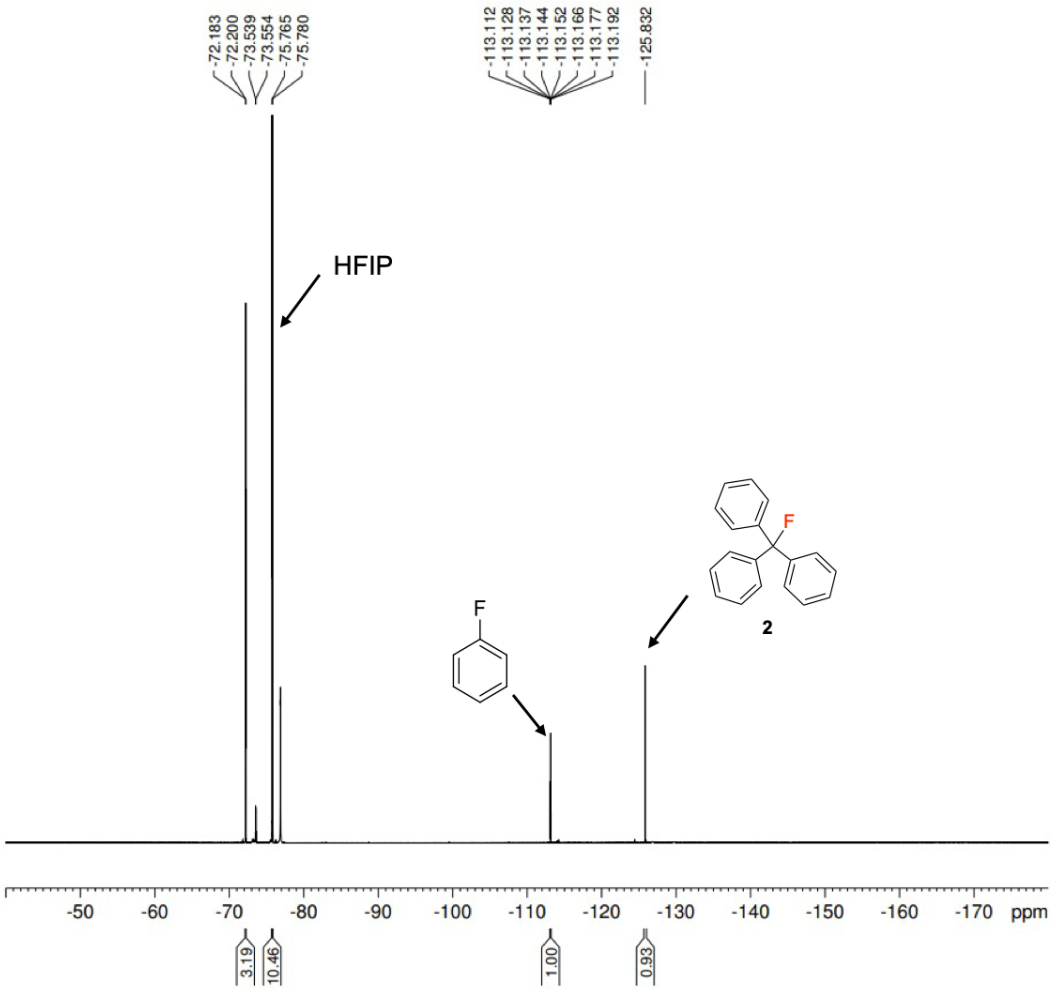

Figure S15. ^{19}F NMR spectrum (376.31 MHz, CD_3CN, 25 °C) of crude reaction mixture of **2**.

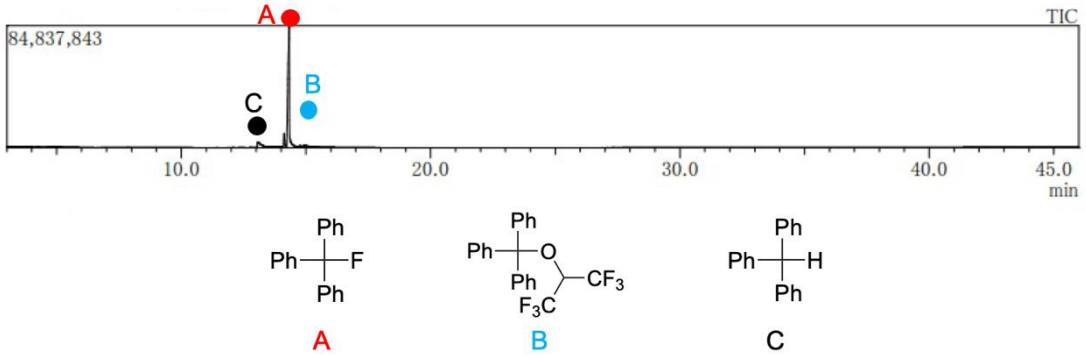

Figure S16. GC-MS of the crude reaction mixture of **2**.

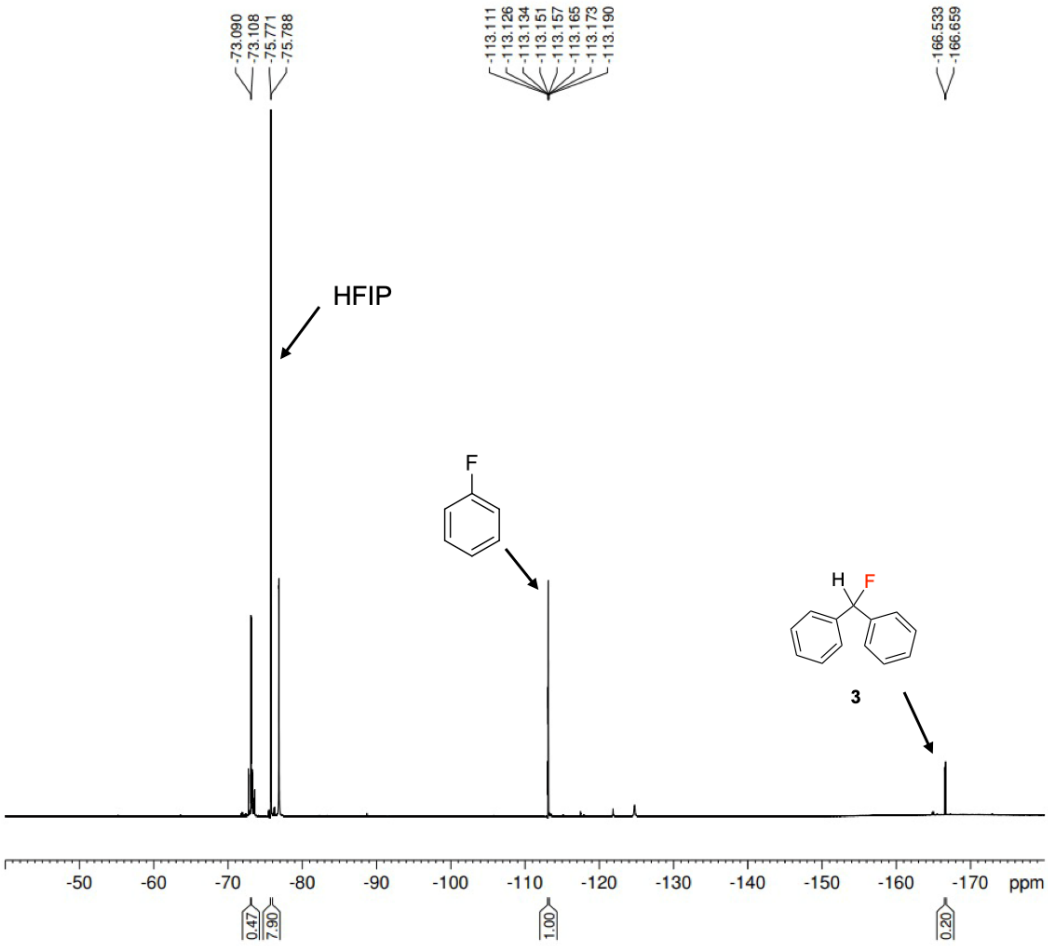

Figure S17. ^{19}F NMR spectrum (376.31 MHz, CD_3CN, 25 °C) of crude reaction mixture of **3**.

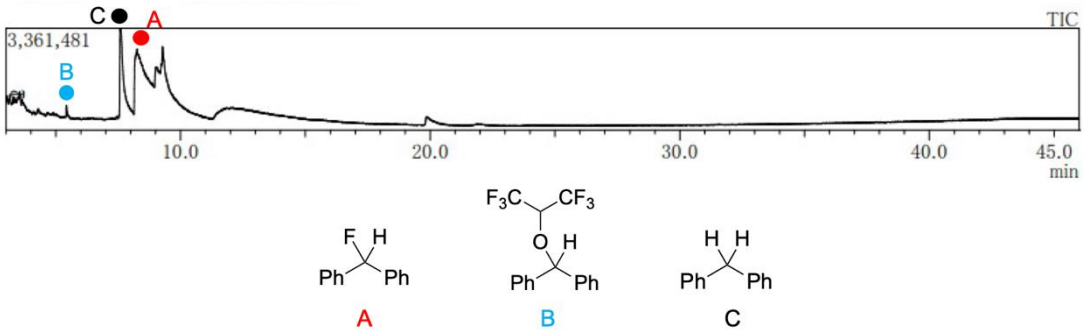

Figure S18. GC-MS of the crude reaction mixture of **3**.

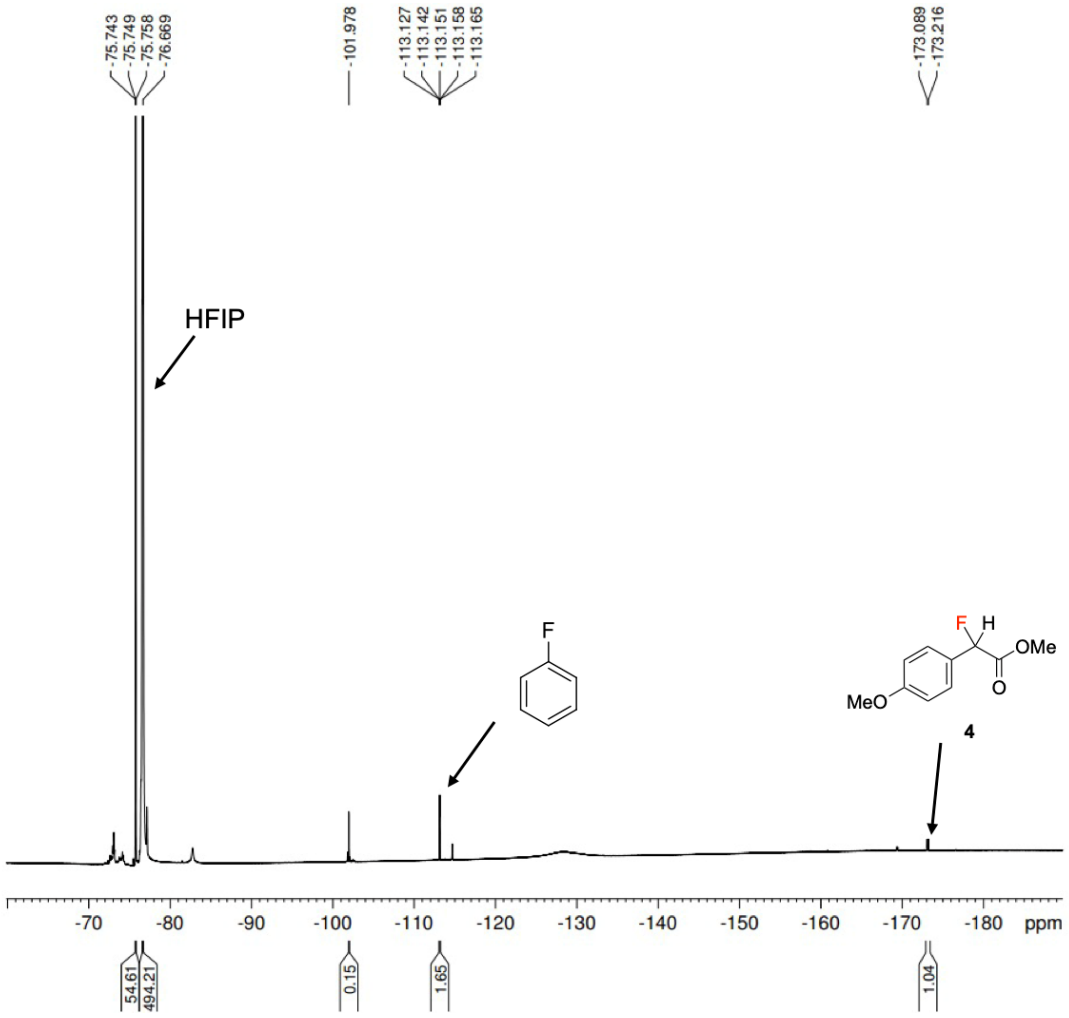

Figure S19. ^{19}F NMR spectrum (376.31 MHz, CD_3CN, 25 °C) of crude reaction mixture of **4**.

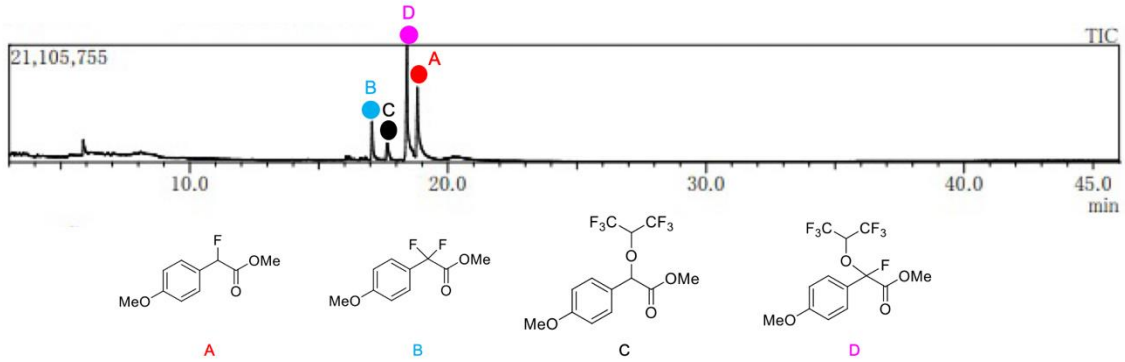

Figure S20. GC-MS of the crude reaction mixture of **4**.

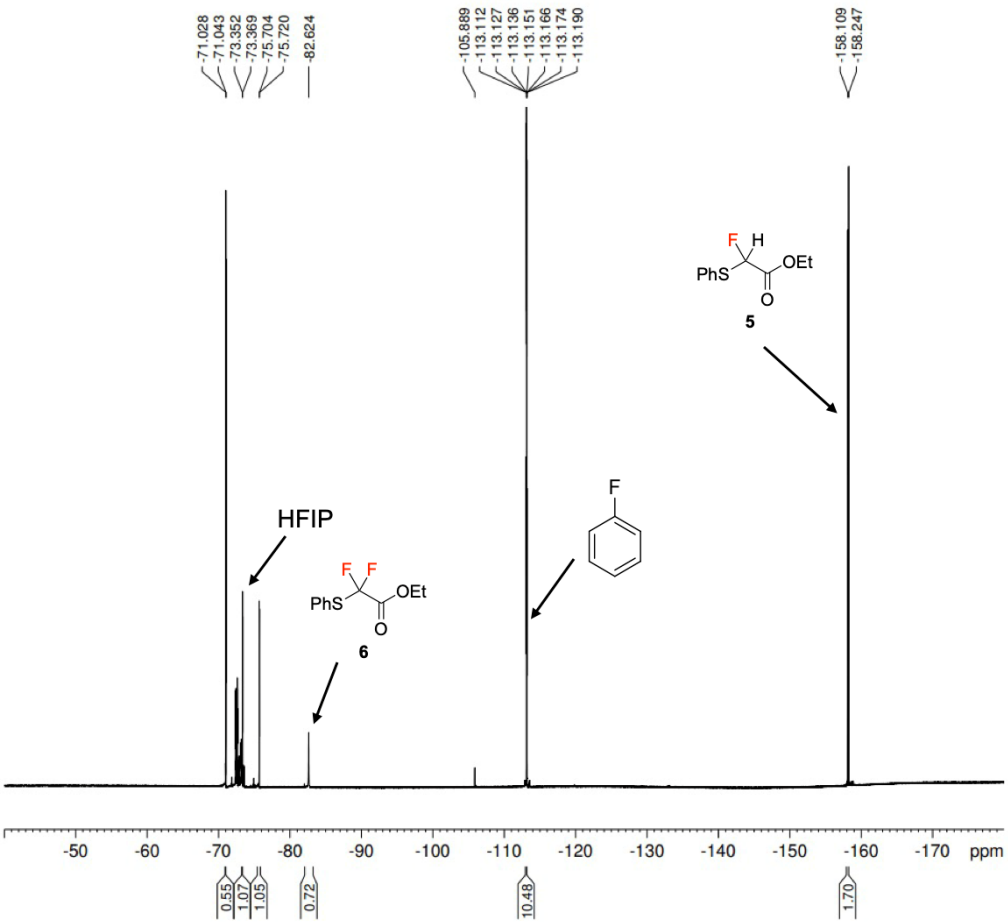

Figure S21. ^{19}F NMR spectrum (376.31 MHz, CD_3CN, 25 °C) of crude raction mixture of **5** and **6**.

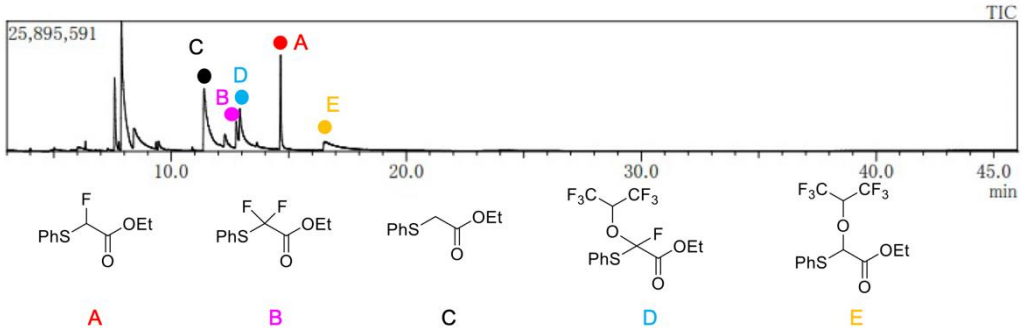

Figure S22. GC-MS of the crude reaction mixture of **5** and **6**.

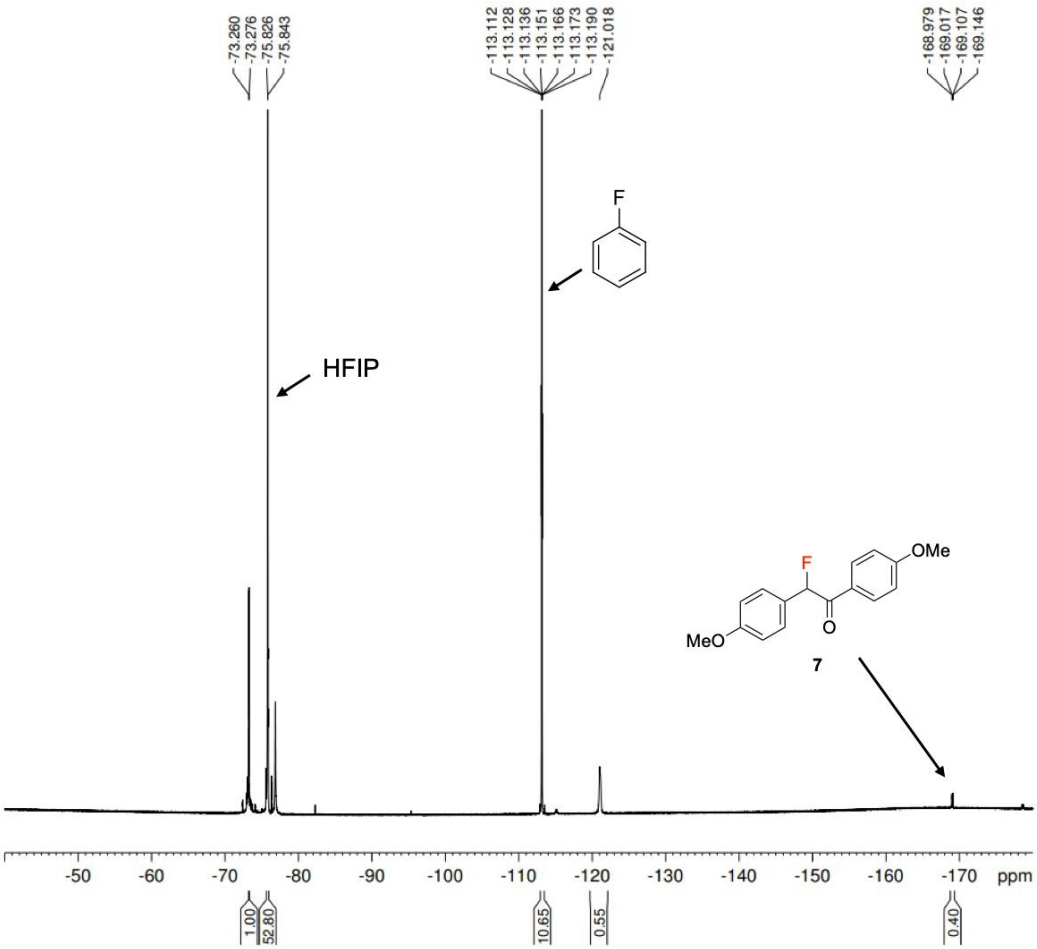

Figure S23. ^{19}F NMR spectrum (376.31 MHz, CD_3CN, 25 °C) of crude reaction mixture of **7**.

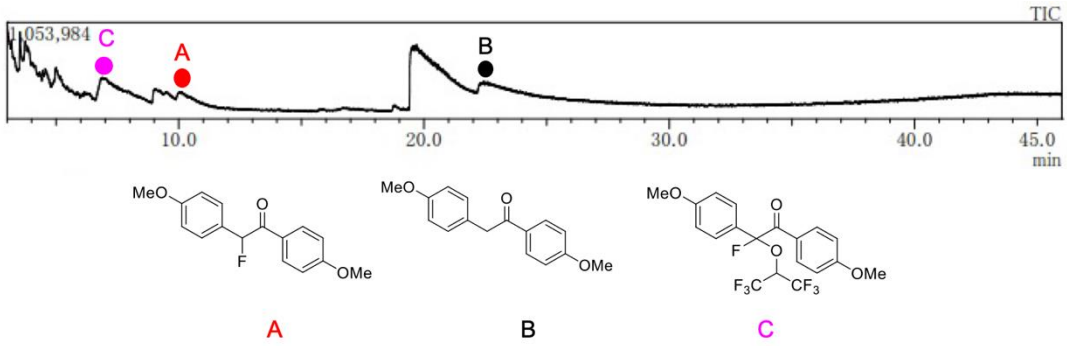

Figure S24. GC-MS of the crude reaction mixture of **7**.

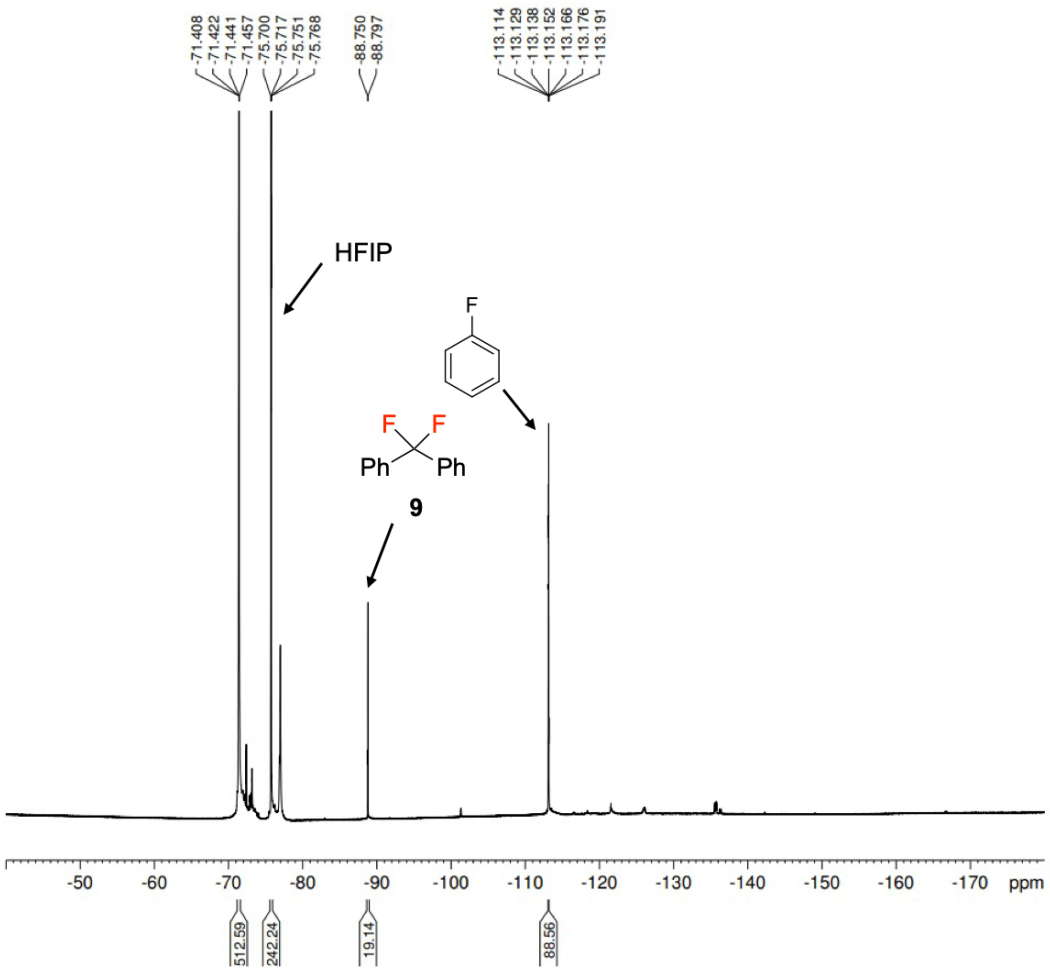

Figure S25. ^{19}F NMR spectrum (376.31 MHz, CD_3CN, 25 °C) of crude material containing **9**.

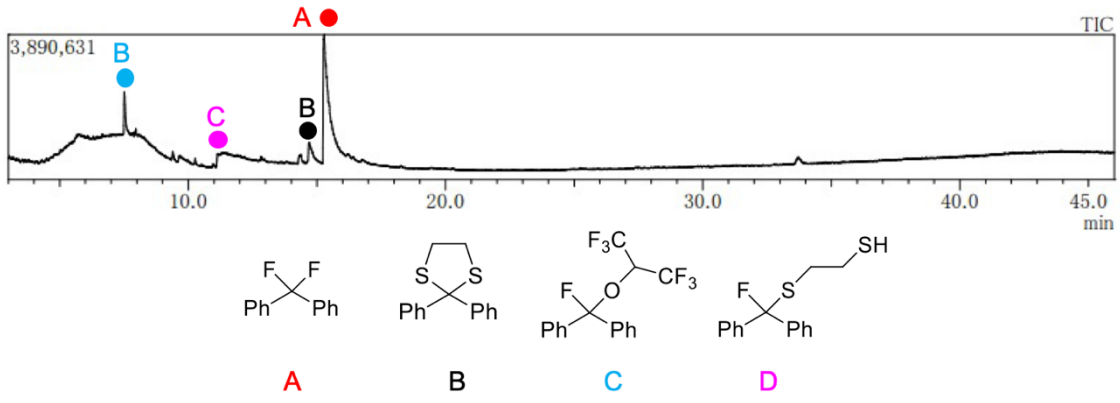

Figure S26. GC-MS of the crude reaction mixture of **9**.